

# NN interaction and spectrum of the light- and medium-mass nuclei using Lattice EFT

---

## Ning Li\*

Facility for Rare Isotope Beams and Department of Physics and Astronomy, Michigan State University, MI 48824, USA

E-mail: [lini@nscl.msu.edu](mailto:lini@nscl.msu.edu)

## Serdar Elhatisari

Helmholtz-Institut für Strahlen- und Kernphysik and Bethe Center for Theoretical Physics, Universität Bonn, D-53115 Bonn, Germany

Department of Physics, Karamanoglu Mehmetbey University, Karaman 70100, Turkey

E-mail: [selhatisari@gmail.com](mailto:selhatisari@gmail.com)

## Evgeny Epelbaum

Institut für Theoretische Physik II, Ruhr-Universität Bochum, D-44870 Bochum, Germany

E-mail: [evgeny.epelbaum@ruhr-uni-bochum.de](mailto:evgeny.epelbaum@ruhr-uni-bochum.de)

## Dean Lee

Facility for Rare Isotope Beams and Department of Physics and Astronomy, Michigan State University, MI 48824, USA

Department of Physics, North Carolina State University, Raleigh, NC 27695, USA

E-mail: [leed@nscl.msu.edu](mailto:leed@nscl.msu.edu)

## Bing-Nan Lu

Facility for Rare Isotope Beams and Department of Physics and Astronomy, Michigan State University, MI 48824, USA

E-mail: [lub@nscl.msu.edu](mailto:lub@nscl.msu.edu)

## Ulf-G. Meißner

Helmholtz-Institut für Strahlen- und Kernphysik and Bethe Center for Theoretical Physics, Universität Bonn, D-53115 Bonn, Germany

Institute for Advanced Simulation, Institut für Kernphysik, and

Jülich Center for Hadron Physics, Forschungszentrum Jülich, D-52425 Jülich, Germany

JARA - High Performance Computing, Forschungszentrum Jülich, D-52425 Jülich, Germany

E-mail: [meissner@hiskp.uni-bonn.de](mailto:meissner@hiskp.uni-bonn.de)

We present a new lattice formulation of chiral nuclear forces which is much more efficient than the one we used in our previous calculations. We also present some preliminary results of nuclear binding for the light- and medium-mass nuclei. Our results provide a pathway to *ab initio* lattice calculations of nuclear structure, reactions, and thermodynamics with accurate and systematic control over the chiral nucleon-nucleon force.

*The 9th International workshop on Chiral Dynamics*

17-21 September 2018

Durham, NC, USA

---

\*Speaker.

## 1. Introduction

In the past fifteen years, it has been witnessed that the nuclear lattice effective field theory has achieved great success in researches of the structure and scattering of atomic nuclei [1, 2, 3, 4, 5, 6]. However, the treatment of nuclear forces at higher orders in the chiral EFT expansion is more difficult on the lattice due to the breaking of rotational invariance produced by nonzero lattice spacing [7, 8]. Fitting the unknown coefficients of the short-range lattice interactions to empirical phase shifts can introduce significant uncertainties. We proposed a new lattice formulation of the chiral nuclear forces to solve this problem. For the new lattice interaction, the angular dependence of the relative separation between the two nucleons is prescribed by spherical harmonics, and the dependence on the nucleon spins is given by the spin-orbit Clebsch-Gordan coefficients. We will show that the neutron-proton scattering phase shifts are produced more accurately with the new lattice interactions than those in our previous calculations.

## 2. Lattice Hamiltonian

In the calculation, the normal-ordered transfer matrix is defined as

$$M =: \exp[-H\alpha_t] :, \quad (2.1)$$

where the  $::$  symbols denote normal ordering where the annihilation operators are on the right and creation operators are on the left.  $\alpha_t = a_t/a$  is the ratio between the temporal lattice spacing,  $a_t$ , and the spacial lattice spacing,  $a$ .

The lattice Hamiltonian  $H$  is formed by a free Hamiltonian, short-range interactions, and long-range interactions,

$$H = H_{\text{free}} + V_{2N}^{\text{short}} + V_{2N}^{\text{long}}. \quad (2.2)$$

### 2.1 Free Hamiltonian

For the free Hamiltonian we use an  $O(a^4)$ -improved action of the form [9],

$$\begin{aligned} H_{\text{free}} = & \frac{49}{12m_N} \sum_{\mathbf{n}} a^\dagger(\mathbf{n})a(\mathbf{n}) - \frac{3}{4m_N} \sum_{\mathbf{n},i} \sum_{\langle \mathbf{n}' \mathbf{n} \rangle_i} a^\dagger(\mathbf{n}')a(\mathbf{n}) \\ & + \frac{3}{40m_N} \sum_{\mathbf{n},i} \sum_{\langle\langle \mathbf{n}' \mathbf{n} \rangle\rangle_i} a^\dagger(\mathbf{n}')a(\mathbf{n}) - \frac{1}{180m_N} \sum_{\mathbf{n},i} \sum_{\langle\langle\langle \mathbf{n}' \mathbf{n} \rangle\rangle\rangle_i} a^\dagger(\mathbf{n}')a(\mathbf{n}), \end{aligned} \quad (2.3)$$

where  $m_N$  is the nucleon mass.

### 2.2 Short-range interactions

Up to next-to-next-to-next-to-leading order in chiral effective field theory, the short-range nucleon-nucleon interaction reads,

$$V_{2N}^{\text{short}} = V_{\text{contact}}^{(Q/\Lambda_\chi)^0} + V_{\text{contact}}^{(Q/\Lambda_\chi)^2} + V_{\text{contact}}^{(Q/\Lambda_\chi)^4}. \quad (2.4)$$

At leading order, we have two non-locally smeared contact operators saturating the two lowest partial waves,

$$V_{\text{contact}}^{(Q/\Lambda_\chi)^0} = C_{1S_0}^{(Q/\Lambda_\chi)^0} V_{1S_0, (Q/\Lambda_\chi)^0} + C_{3S_1}^{(Q/\Lambda_\chi)^0} V_{3S_1, (Q/\Lambda_\chi)^0}, \quad (2.5)$$

where

$$V_{1S_0,(Q/\Lambda_\chi)^0} = \sum_{I_z=-1,0,1} \left[ O_{0,0,0,0,1,I_z}^{0,S_{NL}}(\mathbf{n}) \right]^\dagger O_{0,0,0,0,1,I_z}^{0,S_{NL}}(\mathbf{n}), \quad (2.6)$$

and

$$V_{3S_1,(Q/\Lambda_\chi)^0} = \sum_{J_z=-1,0,1} \left[ O_{1,0,1,J_z,0,0}^{0,S_{NL}}(\mathbf{n}) \right]^\dagger O_{1,0,1,J_z,0,0}^{0,S_{NL}}(\mathbf{n}). \quad (2.7)$$

The contact operators at orders  $(Q/\Lambda_\chi)^2$  and  $(Q/\Lambda_\chi)^4$  can be written in a similar manner, refer to [10] for the specific expressions.

We also include an SU(4)-invariant short-range operator at LO which is very important for nuclear binding [5, 11],

$$V_{\text{SU}(4)} = \frac{C_{\text{SU}(4)}}{2} : \sum_{\mathbf{n}', \mathbf{n}, \mathbf{n}''} \sum_{i', j'} a_{i', j'}^{S_{NL}\dagger}(\mathbf{n}') a_{i', j'}^{S_{NL}}(\mathbf{n}') f_{S_L}(\mathbf{n}' - \mathbf{n}) f_{S_L}(\mathbf{n} - \mathbf{n}'') \sum_{i'', j''} a_{i'', j''}^{S_{NL}\dagger}(\mathbf{n}'') a_{i'', j''}^{S_{NL}}(\mathbf{n}'') :, \quad (2.8)$$

where the smearing function  $f_{S_L}(\mathbf{n})$  is defined as

$$f_{S_L} = \begin{cases} 1, & |\mathbf{n}| = 0, \\ s_L, & |\mathbf{n}| = 1, \\ 0, & \text{otherwise.} \end{cases} \quad (2.9)$$

The index  $i$  corresponds to nucleon spin while  $j$  corresponds to nucleon isospin. The dressed creation operator  $a^{S_{NL}\dagger}$  and annihilation operator  $a^{S_{NL}}$  are defined respectively as

$$a_{i,j}^{S_{NL}}(\mathbf{n}) = a_{i,j}(\mathbf{n}) + s_{NL} \sum_{|\mathbf{n}'|=1} a_{i,j}(\mathbf{n} + \mathbf{n}'), \quad (2.10)$$

and

$$a_{i,j}^{S_{NL}\dagger}(\mathbf{n}) = a_{i,j}^\dagger(\mathbf{n}) + s_{NL} \sum_{|\mathbf{n}'|=1} a_{i,j}^\dagger(\mathbf{n} + \mathbf{n}'). \quad (2.11)$$

The dressed creation (annihilation) operator is used to create (annihilate) not only the nucleon placed at the exact lattice site but also the nucleons located at its nearest-neighbor lattice sites. In this manner, some of the lattice artifacts induced by the nonzero lattice spacing can be removed.

### 2.3 Long-range interactions

In chiral effective field theory, the long-range nucleon-nucleon interaction arise from the pion-exchange potential,

$$V_{2N}^{\text{long}} = V_{\text{OPE}}^{(Q/\Lambda_\chi)^0} + V_{\text{TPE}}^{(Q/\Lambda_\chi)^2} + V_{\text{TPE}}^{(Q/\Lambda_\chi)^3} + V_{\text{TPE}}^{(Q/\Lambda_\chi)^4}. \quad (2.12)$$

The one-pion exchange potential  $V_{\text{OPE}}$  has the form

$$V_{\text{OPE}} = -\frac{g_A^2}{8F_\pi^2} \sum_{\mathbf{n}', \mathbf{n}, S', S, I} : \rho_{S', I}(\mathbf{n}') f_{S'S}(\mathbf{n}' - \mathbf{n}) \rho_{S, I}(\mathbf{n}) :, \quad (2.13)$$

where  $f_{S'S}$  is defined as

$$f_{S'S}(\mathbf{n}' - \mathbf{n}) = \frac{1}{L^3} \sum_{\mathbf{q}} \frac{Q(q_{S'}) Q(q_S) \exp[-i\mathbf{q} \cdot (\mathbf{n}' - \mathbf{n}) - b_\pi(\mathbf{q}^2 + M_\pi^2)]}{\mathbf{q}^2 + M_\pi^2}, \quad (2.14)$$

and each lattice momentum component  $q_S$  is an integer multiplied by  $2\pi/L$ . The specific expressions of the two-pion-exchange potentials at NLO, N2LO, and N3LO can be found in [10].

### 3. Galilean Invariance Restoration (GIR)

Due to the nonlocal smearing parameter  $s_{NL}$  we use to construct the non-locally smeared operators and the lattice artifacts, the Galilean invariance is breaking for the new lattice interaction. To restore the Galilean invariance, we introduce the Galilean invariance restoration terms for each partial wave channels. For example, the GIR operator for the  $^1S_0$  channel reads [12]

$$\begin{aligned}
V_{GIR}^{^1S_0} = & C_{GIR,0}^{^1S_0} \sum_{\mathbf{n}} \sum_{J_z=-1,0,1} \left[ O_{0,0,0,0,1,J_z}^{0,s_{NL}}(\mathbf{n}) \right]^\dagger O_{0,0,0,0,1,J_z}^{0,s_{NL}}(\mathbf{n}) \\
& + C_{GIR,1}^{^1S_0} \sum_{\mathbf{n}} \sum_{|\mathbf{n}'|=1} \sum_{J_z=-1,0,1} \left[ O_{0,0,0,0,1,J_z}^{0,s_{NL}}(\mathbf{n}+\mathbf{n}') \right]^\dagger O_{0,0,0,0,1,J_z}^{0,s_{NL}}(\mathbf{n}) \\
& + C_{GIR,2}^{^1S_0} \sum_{\mathbf{n}} \sum_{|\mathbf{n}'|=\sqrt{2}} \sum_{J_z=-1,0,1} \left[ O_{0,0,0,0,1,J_z}^{0,s_{NL}}(\mathbf{n}+\mathbf{n}') \right]^\dagger O_{0,0,0,0,1,J_z}^{0,s_{NL}}(\mathbf{n}), \quad (3.1)
\end{aligned}$$

whereas that for the  $^1P_1$  channel is

$$\begin{aligned}
V_{GIR}^{^1P_1} = & C_{GIR,0}^{^1P_1} \sum_{\mathbf{n}} \sum_{J_z=-1,0,1} \left[ O_{0,1,1,J_z,0,0}^{0,s_{NL}}(\mathbf{n}) \right]^\dagger O_{0,1,1,J_z,0,0}^{0,s_{NL}}(\mathbf{n}) \\
& + C_{GIR,1}^{^1P_1} \sum_{\mathbf{n}} \sum_{|\mathbf{n}'|=1} \sum_{J_z=-1,0,1} \left[ O_{0,1,1,J_z,0,0}^{0,s_{NL}}(\mathbf{n}+\mathbf{n}') \right]^\dagger O_{0,1,1,J_z,0,0}^{0,s_{NL}}(\mathbf{n}) \\
& + C_{GIR,2}^{^1P_1} \sum_{\mathbf{n}} \sum_{|\mathbf{n}'|=\sqrt{2}} \sum_{J_z=-1,0,1} \left[ O_{0,1,1,J_z,0,0}^{0,s_{NL}}(\mathbf{n}+\mathbf{n}') \right]^\dagger O_{0,1,1,J_z,0,0}^{0,s_{NL}}(\mathbf{n}). \quad (3.2)
\end{aligned}$$

Using these GIR operators, we can restore Galilean invariance for each channel by finely tuning  $C_{GIR,i}$  ( $i = 0, 1, 2$ ) with the constraint,

$$C_{GIR,0} + 6C_{GIR,1} + 12C_{GIR,2} = 0, \quad (3.3)$$

which is the requirement that the GIR correction should be vanishing for zero total momentum.

### 4. Scattering on the lattice

In our calculation, we use two different approaches to calculate the neutron-proton scattering phase shifts, the Lüscher's formula and the spherical wall method.

#### 4.1 Lüscher's formula

In [13], Lüscher derived a simple formula connecting the two-body S-wave scattering phase shift  $\delta_0$  with the energy levels calculated in the lattice framework, which reads

$$\exp(2i\delta_0(k)) = \frac{\zeta_{00}(1; q^2) + i\pi^{3/2}q}{\zeta_{00}(1; q^2) - i\pi^{3/2}q}, \quad (4.1)$$

where

$$q = \frac{kL}{2\pi}, \quad (4.2)$$

and

$$\zeta_{00}(s; q^2) = \frac{1}{\sqrt{4\pi}} \sum_{\mathbf{n} \in \mathbb{Z}^3} (\mathbf{n}^2 - q^2)^{-s} \quad (4.3)$$

is the zeta function which is convergent when  $\text{Re}(s) > 3/2$ , and can be analytically continued to  $s = 1$ . Later, this formula was generalized to moving frames with center-of-mass momentum  $\mathbf{P} = (2\pi/L)\mathbf{k}$  [14, 15, 16],

$$\delta_0(k) = \arctan \left( \frac{\gamma q \pi^{3/2}}{\zeta_{00}^{\mathbf{d}}(1; q^2)} \right) \quad (4.4)$$

where

$$\zeta_{00}^{\mathbf{d}}(s; q^2) = \frac{1}{\sqrt{4\pi}} \sum_{\mathbf{r} \in P_{\mathbf{d}}} (\mathbf{r}^2 - q^2)^{-s}, \quad (4.5)$$

is the generalized zeta function. The summation region  $P_{\mathbf{d}}$  is defined as

$$P_{\mathbf{d}} = \{ \mathbf{r} \in \mathbb{R}^3 | \mathbf{r} = \gamma^{-1}(\mathbf{n} + \mathbf{d}/2), \mathbf{n} \in \mathbb{Z}^3 \}, \quad (4.6)$$

where  $\gamma$  is the Lorentz factor and  $\gamma^{-1}\mathbf{n}$  is the shorthand notation for  $\gamma^{-1}\mathbf{n}_{\parallel} + \mathbf{n}_{\perp}$ .

## 4.2 Spherical wall method

To calculate the scattering phase shifts and mixing angles using the spherical wall method, we first construct radial wave functions through the spherical harmonics with quantum numbers  $(l, l_z)$  [17, 18],

$$|r\rangle^{l, l_z} = \sum_{\tilde{r}'} Y_{l, l_z}(\tilde{r}') \delta_{|\tilde{r}'|=r} |\mathbf{r}'\rangle, \quad (4.7)$$

where  $\tilde{r}'$  runs over all lattice sites having the same radial lattice distance. Using this definition for the radial wave function, the Hamiltonian matrix over a three-dimensional lattice can be reduced to a one-dimensional radial Hamiltonian,  $H_{\mathbf{r}, \mathbf{r}'} \rightarrow H_{r, r'}$ .

The phase shifts and mixing angles can be extracted from the radial wave function in the region where the NN force is vanishing. In this range, the wave function is a superposition of the incoming plane wave and outgoing radial wave which can be expanded as [17, 10]

$$\langle r | k, l \rangle = A_j h_l^{(1)}(kr) + B_j h_l^{(2)}(kr), \quad (4.8)$$

where  $h_l^{(1)}(kr)$  and  $h_l^{(2)}(kr)$  are the spherical Hankel functions.  $k = \sqrt{2\mu E}$  with  $\mu$  the reduced mass and  $E$  the relative energy of the two-nucleon system. The scattering coefficients  $A_j$  and  $B_j$  satisfy the relations,

$$B_j = S_j A_j, \quad (4.9)$$

where  $S_j = \exp(2i\delta_j)$  is the  $S$ -matrix and  $\delta_j$  is the phase shift. The phase shift is determined by setting

$$\delta_j = \frac{1}{2i} \log \left( \frac{B_j}{A_j} \right). \quad (4.10)$$

In the case of the coupled channels with  $j > 0$ , both of the coupled partial waves,  $l = j - 1$  and  $l = j + 1$ , satisfy Eq. (4.9), and the  $S$ -matrix couples the two channels together. Throughout this work we adopt the so-called Stapp parameterization of the phase shifts and mixing angles for the coupled channels [19],

$$S = \begin{bmatrix} \cos(2\varepsilon) \exp(2i\delta_{j-1}^{1j}) & i \sin(2\varepsilon) \exp(i\delta_{j-1}^{1j} + i\delta_{j+1}^{1j}) \\ i \sin(2\varepsilon) \exp(i\delta_{j-1}^{1j} + i\delta_{j+1}^{1j}) & \cos(2\varepsilon) \exp(2i\delta_{j+1}^{1j}) \end{bmatrix}. \quad (4.11)$$

## 5. Neutron-proton scattering phase shifts

### 5.1 S-wave neutron-proton scattering phase shifts using Lüscher's formula

To obtain results for a wide energy range, we use several cubic boxes with volumes  $V = (14a)^3$ ,  $(16a)^3$ , and  $(18a)^3$ . To study the finite volume effects, larger cubic boxes with volume of  $V = (24a)^3$ ,  $(26a)^3$  and  $(28a)^3$  are also used for the same calculations. We first perform the calculation in the rest-frame, and then boost the proton-neutron system to moving frames with momenta  $\mathbf{P} = (2\pi/L)\mathbf{k}$ . The results for  $^1S_0$  and  $^3S_1$  are shown in Figs. 1 and 2, respectively. The plots in top row are the LO results while those in the bottom row are the N3LO results. The left two columns are the results using the smaller boxes whereas the right two columns are the results using the larger boxes. ‘w/o’ means without GIR corrections whereas ‘w/’ denotes the results after restoring the Galilean invariance.

Our results indicate that there are small Galilean invariance breaking effects for the new lattice formulation due to the nonlocal smearing and lattice artifacts. The Galilean invariance can be restored after including the Galilean invariance restoration operators.

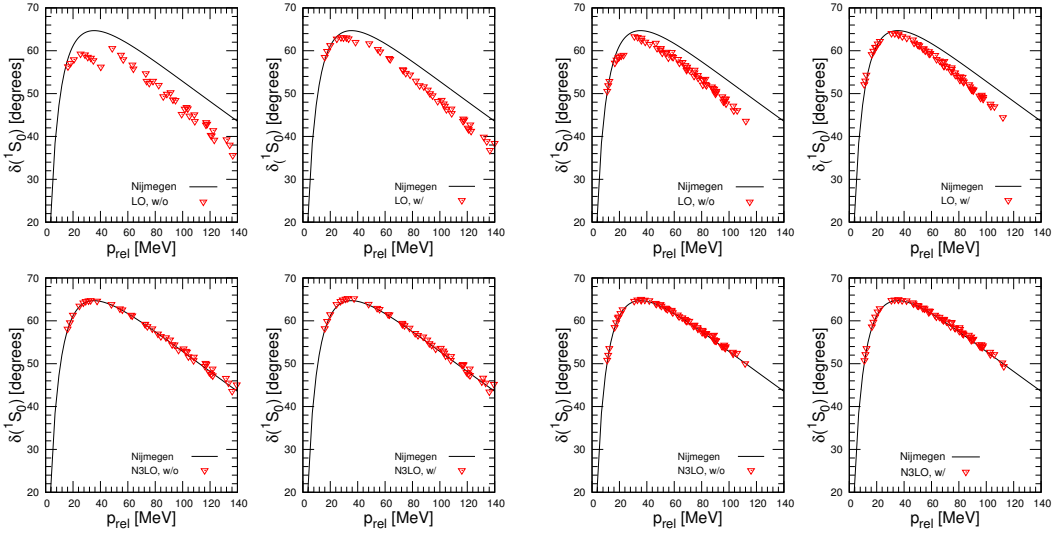


**Figure 1:** (Color online) Neutron-proton scattering phase shifts of  $^1S_0$  as a function of the relative momenta between the proton and neutron. The Lüscher formula is used to extract the scattering phase shifts. Refer to the text for an explanation of the difference between different plots.

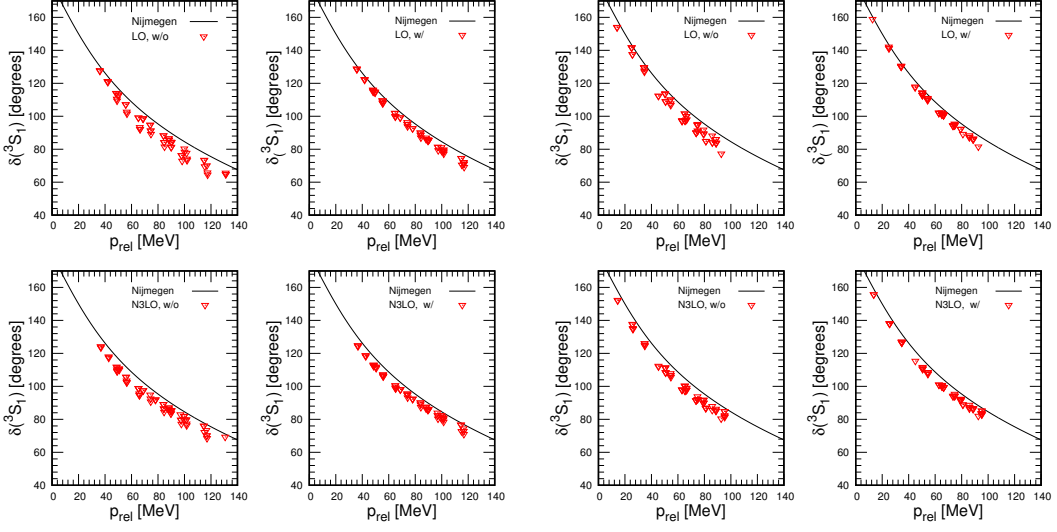


**Figure 2:** (Color online) Neutron-proton scattering phase shifts of  ${}^3S_1$  as a function of the relative momenta between the proton and neutron. The Lüscher formula is used to extract the scattering phase shifts. Refer to the text for an explanation of the difference between different plots.

## 5.2 Neutron-proton scattering phase shifts using spherical wall method

In Fig. (3), we show the neutron-proton scattering phase shifts calculated using the spherical wall method. To calculate the estimated theoretical uncertainties, we follow the prescription in Refs. [20, 21] where the theoretical uncertainty for some observable  $X(p)$  at order  $N^m\text{LO}$  and momentum  $p$  is given by

$$\Delta X^{N^m\text{LO}}(p) = \max \left( Q^{m+2} |X^{\text{LO}}(p)|, Q^m |X^{\text{LO}}(p) - X^{\text{NLO}}(p)|, \dots, Q^1 |X^{N^{m-1}\text{LO}}(p) - X^{N^m\text{LO}}(p)| \right). \quad (5.1)$$

Our results indicate that with only a few exceptions, the error bands for each order generally overlap with each other and cover the empirical phase shifts, which provides a promising sign of convergence of the chiral effective field theory expansion on the lattice.

## 6. Spectrum of the light and medium-mass nuclei

We calculate the nuclear binding of the light- and medium-mass nuclei using the new lattice interaction, and provide some preliminary results in Fig. (4) [22]. From the results, one can see that the binding energy of the light nuclei are much more accurate than our previous calculations. We should emphasize that in these calculations only the two-body interaction is applied. Hopefully, these discrepancy can be fixed by including the three-body interaction. Such calculations are undergo.

## 7. Summary and outlook

We have proposed a new lattice formulation of the chiral NN force which is more efficient than the one we used in our previous calculations. The results are more accurate. We also calculate

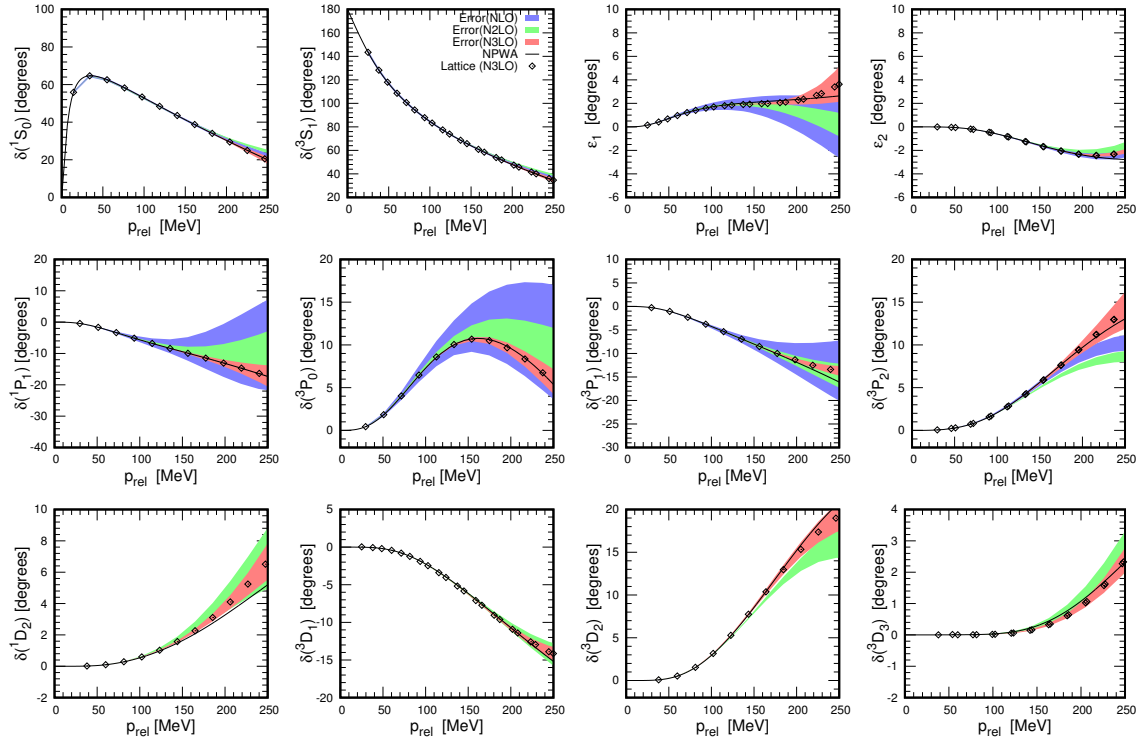


**Figure 3:** (Color online) The neutron-proton scattering phase shifts and mixing angles versus the relative momenta. The black solid line and diamonds denote the phase shift or mixing angle from the Nijmegen partial-wave analysis (NPWA) and lattice calculation at  $N^3\text{LO}$ , respectively. See the text for an explanation of the error bands.

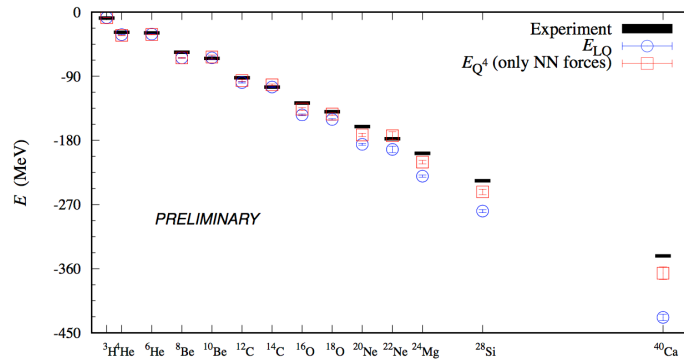


**Figure 4:** Spectrum of the light and medium-mass nuclei. In the calculations only the two-body interactions are applied.



the binding energy of the light- and medium-mass nuclei, the results are promising. In summary, the new lattice interactions are far more efficient and accurate in reproducing physical data than previous lattice interactions. It is very helpful for our future Monte Carlo simulations.

## References

- [1] E. Epelbaum, H. Krebs, D. Lee and U.-G. Meißner, *Ab initio calculation of the Hoyle state*, *Phys. Rev. Lett.* **106** (2011) 192501 [1101.2547].
- [2] E. Epelbaum, H. Krebs, T. Lähde, D. Lee and U.-G. Meißner, *Structure and rotations of the Hoyle state*, *Phys. Rev. Lett.* **109** (2012) 252501 [1208.1328].
- [3] E. Epelbaum, H. Krebs, T. A. Lähde, D. Lee, U.-G. Meißner and G. Rupak, *Ab initio calculation of the spectrum and structure of  $^{16}\text{O}$* , *Phys. Rev. Lett.* **112** (2014) 102501 [1312.7703].
- [4] S. Elhatisari, D. Lee, G. Rupak, E. Epelbaum, H. Krebs, T. A. Lähde et al., *Ab initio alpha-alpha scattering*, *Nature* **528** (2015) 111 [1506.03513].
- [5] S. Elhatisari et al., *Nuclear binding near a quantum phase transition*, *Phys. Rev. Lett.* **117** (2016) 132501 [1602.04539].
- [6] S. Elhatisari, E. Epelbaum, H. Krebs, T. A. Lähde, D. Lee, N. Li et al., *Ab initio Calculations of the Isotopic Dependence of Nuclear Clustering*, *Phys. Rev. Lett.* **119** (2017) 222505 [1702.05177].
- [7] J. M. Alarcón, D. Du, N. Klein, T. A. Lähde, D. Lee, N. Li et al., *Neutron-proton scattering at next-to-next-to-leading order in Nuclear Lattice Effective Field Theory*, *Eur. Phys. J.* **A53** (2017) 83 [1702.05319].
- [8] N. Klein, S. Elhatisari, T. A. Lähde, D. Lee and U.-G. Meißner, *The Tjon Band in Nuclear Lattice Effective Field Theory*, *Eur. Phys. J.* **A54** (2018) 121 [1803.04231].
- [9] D. Lee, *Lattice simulations for few- and many-body systems*, *Prog. Part. Nucl. Phys.* **63** (2009) 117 [0804.3501].
- [10] N. Li, S. Elhatisari, E. Epelbaum, D. Lee, B.-N. Lu and U.-G. Meißner, *Neutron-proton scattering with lattice chiral effective field theory at next-to-next-to-next-to-leading order*, *Phys. Rev.* **C98** (2018) 044002 [1806.07994].
- [11] B.-N. Lu, N. Li, S. Elhatisari, D. Lee, E. Epelbaum and U.-G. Meißner, *Essential elements for nuclear binding*, 1812.10928.
- [12] N. Li, S. Elhatisari, E. Epelbaum, D. Lee, B.-N. Lu and U.-G. Meißner, *Galilean invariance restoration on the lattice*, 1902.01295.
- [13] M. Lüscher, *Two particle states on a torus and their relation to the scattering matrix*, *Nucl. Phys.* **B354** (1991) 531.
- [14] K. Rummukainen and S. A. Gottlieb, *Resonance scattering phase shifts on a nonrest frame lattice*, *Nucl. Phys.* **B450** (1995) 397 [hep-lat/9503028].
- [15] S. R. Beane, P. F. Bedaque, A. Parreno and M. J. Savage, *Two nucleons on a lattice*, *Phys. Lett.* **B585** (2004) 106 [hep-lat/0312004].
- [16] X. Feng, X. Li and C. Liu, *Two particle states in an asymmetric box and the elastic scattering phases*, *Phys. Rev.* **D70** (2004) 014505 [hep-lat/0404001].

- [17] B.-N. Lu, T. A. Lähde, D. Lee and U.-G. Meißner, *Precise determination of lattice phase shifts and mixing angles*, *Phys. Lett.* **B760** (2016) 309 [1506.05652].
- [18] S. Elhatisari, D. Lee, U.-G. Meißner and G. Rupak, *Nucleon-deuteron scattering using the adiabatic projection method*, *Eur. Phys. J.* **A52** (2016) 174 [1603.02333].
- [19] H. P. Stapp, T. J. Ypsilantis and N. Metropolis, *Phase shift analysis of 310-MeV proton proton scattering experiments*, *Phys. Rev.* **105** (1957) 302.
- [20] E. Epelbaum, H. Krebs and U.-G. Meißner, *Improved chiral nucleon-nucleon potential up to next-to-next-to-next-to-leading order*, *Eur. Phys. J.* **A51** (2015) 53 [1412.0142].
- [21] E. Epelbaum, H. Krebs and U.-G. Meißner, *Precision nucleon-nucleon potential at fifth order in the chiral expansion*, *Phys. Rev. Lett.* **115** (2015) 122301 [1412.4623].
- [22] S. Elhatisari, work in process.